Pharmaceutical Research, Vol. 26, No. 1, January 2009 (© 2008)
DOI: 10.1007/s11095-008-9708-y

Research Paper

Influence of Stabilizers on the Physicochemical Characteristics of Inhaled Insulin Powders Produced by Supercritical Antisolvent Process

Yong Ho Kim,[1] Constantinos Sioutas,[2] and Katherine S. Shing[1,3]

Received July 3, 2008; accepted August 12, 2008; published online September 4, 2008

Purpose. To examine the effect of stabilizers on aerosol physicochemical characteristics of inhaled insulin particles produced using a supercritical fluid technology.
Materials and Methods. Insulin with stabilizers such as mannitol and trehalose was micronized by aerosol solvent extraction system (ASES). The supercritically-micronized insulin particles were characterized for size, shape, aerosol behavior, crystallinity and secondary structure.
Results. Experimental results indicated that when insulin was incorporated with the most commonly used stabilizer mannitol (insulin/mannitol: 15/85 wt.%, designated IM), the particles formed were irregular and needle-shaped and had a tendency to agglomerate. With the incorporation of a second stabilizer trehalose (insulin/mannitol/trehalose: 15/70/15 wt.%, designated IMT), the particles were relatively uniform, more spherical, less cohesive, and less agglomerated in an air flow, when compared to IM particles. The mass median aerodynamic diameter of the IMT particles was 2.32 μm which is suitable for use in inhalation therapy. *In vitro* deposition test using micro-orifice uniform deposit impactor showed 69±7 wt.% of the IMT particles was deposited in stage 3, 4, 5 and 6 while 41±15 wt.% of the IM particles was deposited in the same stages. In terms of insulin stability, secondary structures of insulin particles were not adversely affected by the ASES processing studied here.
Conclusions. When properly formulated (as in IMT particles), ASES process can produce particles with appropriate size and size distribution suitable for pulmonary insulin delivery.

KEY WORDS: insulin; pulmonary delivery; stabilizer; supercritical antisolvent.

INTRODUCTION

Since insulin was shown to be a successful treatment of diabetes in 1922, it has been delivered by only subcutaneous injections for the past 80 years (1,2). Although numerous attempts have been made to develop alternative administrations to the subcutaneous injections, until recently most attempts have met with limited success, except for insulin delivery via pulmonary route. The first inhaled form of insulin, Exubera® (Pfizer Inc., Aventis Pharma, and Nektar Therapeutics) was approved by the US FDA for the treatment of adults with type 1 and type 2 diabetes in 2006. Recent setback in Exubera® is primarily due to the relatively awkward design of the delivery device, and the adverse effect on users whose pulmonary functions have been impaired by lung disease. Although Pfizer had pulled Exubera® from the market in October 2007, there is still room for improvement of inhaled insulin. MannKind, Kos Pharmaceuticals and BioSnate Pharmaceuticals are still actively working on developing an inhaled insulin product (3).

[1] Mork Family Department of Chemical Engineering and Materials Science, University of Southern California, Los Angeles, California 90089-1211, USA.
[2] Department of Civil and Environmental Engineering, University of Southern California, Los Angeles, California 90089-1211, USA.
[3] To whom correspondence should be addressed. (e-mail: shing@usc.edu)

Despite the US FDA approval of inhaled insulin, it is recognized that consistency in lung deposition still needs optimization (4). To achieve consistent and efficient insulin deposition in the lung, several drawbacks must be overcome; losses within the device and environment before insulin is passed into the mouth, deposition in the mouth and throat before insulin reaches the lung and losses in the lung itself (metabolism) after insulin deposits in the lung (5). The factors affecting the efficiency of aerosol insulin include the aerodynamic diameter, surface morphology, formulation, inspiratory flow rate and inhaled volume (6). These factors may be controlled by the development of particle engineering techniques. Particle deposition characteristics depend primarily on its aerodynamic diameter, which is a function of particle size, shape and density (7). Particles larger than 10 μm are deposited in the upper respiratory tract, e.g., mouth, larynx and trachea, whereas particles between 0.1~0.5 μm are exhaled from the lung with a small deposition fraction (8,9). In general, it is widely accepted that the particles with aerodynamic diameters between 2 to 3 μm are most likely to deposit in deep lung (alveolar) region.

In this study, insulin was micronized by using a supercritical fluid (SCF) technology known as aerosol solvent extraction system (ASES) process. Recently, several SCF technologies have been shown to be effective routes for preparing particles for pulmonary drug delivery (10–14). These methods avoid most of the drawbacks of the

conventional micronization techniques such as wide particle size distribution, thermal denaturing, excessive surface charge and roughness (15,16), while offering the advantages of a relatively solvent-free product, the ability to control crystal polymorphism, a mild operating temperature, a single-step process, and they are also environmentally benign (17–20). Typical dry powder formulations of pulmonary delivered insulin combine insulin with additives, of which stabilizers form the majority component (over 60% by weight). Besides stabilizing insulin, the stabilizers also prolong the residence time of insulin at its site of action by reducing clearance, decrease irritation caused by insulin, decrease toxicity due to high initial doses of insulin and improve taste of the product (21). For dry powder inhaler (DPI) formulation, carbohydrates such as mannitol, trehalose, glucose and lactose are often added. Among them, mannitol appears to be the most popular candidate for DPI formulations due to its dispersability properties. When insulin/mannitol particles are precipitated by the ASES process, however, particle shapes are highly irregular and needle-like which may cause low delivery efficiency and poor dose reproducibility even though the particle size is suitable for reaching respiratory regions (22).

The aims of this work were first to show the possibility of modifying the shape of insulin/mannitol particles using an additional stabilizer (trehalose) and then to improve aerosol delivery efficiency by modifying the particle shape with changing the ratio of stabilizers to insulin. The importance of solvent choice was also demonstrated. Insulin particles with stabilizers precipitated by the ASES process were characterized using scanning electron microscopy (SEM), aerodynamic particle sizer (APS) and micro-orifice uniform deposit impactor (MOUDI) in order to examine the aerodynamic particle size and the overall performance of the drug delivery process in an accelerating air flow. Insulin stability was evaluated by secondary structure analysis using Fourier transform infrared (FTIR) spectroscopy. In addition, ultraviolet (UV) spectroscopy, x-ray photoelectron spectroscopy (XPS) and x-ray diffraction (XRD) were used to examine various physical properties of the particles.

MATERIALS AND METHODS

Chemicals and Reagents

Insulin from bovine pancreas (insulin, ≥27 USP units per milligram) was purchased from Sigma-Aldrich (St. Louis, MO, USA). The physical properties of bovine and human insulin are very similar and therefore conclusions in this study are expected to be applicable to both. D-mannitol (purity >99%) was purchased from Sigma-Aldrich (St. Louis, MO, USA) and D(+)-trehalose (purity >99.5%) was purchased from Fluka (Buchs, Switzerland). The solvents *N*, *N*-Dimethylformamide (DMF, purity 99.9%) and Dimethylsulphoxide (DMSO, purity 99.9%) were purchased from Burdick & Jackson (Muskegon, MI, USA) and EMD Chemical Inc. (Gibbstown, NJ, USA), respectively. Carbon dioxide (CO_2, purity 99.8%) was purchased from Gilmore (South El Monte, CA, USA). All of the chemicals were used as received without further purification.

Experimental Procedures

The schematic diagram of the ASES apparatus is shown in Fig. 1. The windowed precipitation vessel (1) was pressurized with CO_2 using a reciprocating pump ((2), Milton Roy, model Minipump). Operating temperatures were maintained by the air heated-bath ((3), Ruska, model 2320) and a heat exchanger connected to an auxiliary thermostatic bath ((4), Haake, model A82). The temperature was measured by a K-type thermocouple ((5), Omega, model TJ36-CASS-18G-12) and digital indicator (Omega, model CN132) with an accuracy of±0.1°C. The vessel pressure was controlled by a back-pressure regulator ((6), Tescom, model 26-IN62–24), heated by a heating tape ((7), Barnstead, model BS0051-020) to prevent plugging in the valve due to CO_2 depressurization. The pressure in the vessel is measured using a dial pressure gauge ((8), Heise, model CMM 55214). After steady pressure, temperature, and CO_2 flow rate were achieved, the solution containing insulin and stabilizers was injected co-currently with the CO_2 into the precipitation vessel through a 127 μm internal diameter stainless steel capillary tubing, ((9), Supelco, model 56720-U) using a computer controlled syringe pump ((10), ISCO, model 100D). For this study, the CO_2 flow rate was fixed at 1.5 SLPM (standard liter per minute). The CO_2 was continuously fed through the vessel at constant flow rate controlled by the fine metering valve ((11), Hoke, model 1315G2Y) and by adjusting the power of the pump. The CO_2 flow rate was measured with a rotameter ((12), Matheson, model KIT-0150-AO) and a dry gas meter ((13), Apex, model SK25). At the end of each experiment, the flow of insulin/stabilizer solution was stopped, and fresh CO_2 added to the precipitation vessel to wash and dry the precipitated particles. After washing was complete, a small amount of CO_2 was

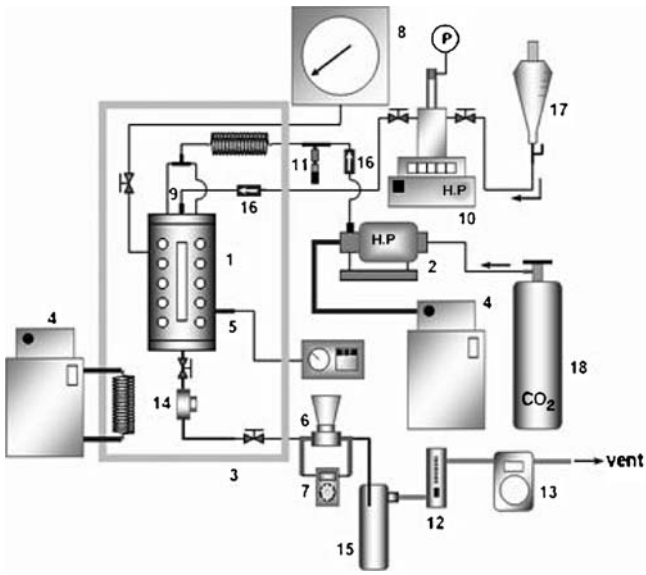

Fig. 1. The experimental apparatus used for ASES process. (*1*) precipitation vessel, (*2*) high pressure pump, (*3*) air bath, (*4*) refrigerated circulator, (*5*) thermo couple, (*6*) back pressure regulator, (*7*) heating controller, (*8*) pressure gauge, (*9*) nozzle (ID 127 μm), (*10*) high pressure pump, (*11*) metering valve, (*12*) rotameter, (*13*) gas meter, (*14*) metal filter (0.5 μm), (*15*) separator, (*16*) check valve, (*17*) drug solution reservoir, (*18*) liquid CO_2.

vented through the nozzle to remove any remaining solution, and then most CO_2 was purged through a back-pressure regulator. The vessel was then depressurized, and the precipitated particles were collected at the bottom of the vessel where a metal filter ((14), Swagelok, model SS-4TF-05) prevents venting of the precipitated particles. A range of operating pressures (100~200 bar) and fixed temperature (35°C) was applied to produce micronized insulin/stabilizer particles using the ASES process.

Scanning Electron Microscopy

The morphology and the surface characteristics of the precipitated drug particles were examined using SEM (Cambridge, model 360). The particles were fixed by double-sided conductive adhesive tape (Ted pella) on the aluminum stub and covered with gold under an argon atmosphere (40 Pa) at 50 μA for 60 s using a sputter coater (Ernest F. Fullam, model EMS-76M).

Aerodynamic Particle Sizer

Particle size distributions (PSD) of the produced particles in an accelerated air stream were measured by APS (TSI Inc., model 3321), which operates on time-of-flight and light-scattering intensity principles (23). A small amount of particles, about 3 mg, produced in this work were loaded into a dry powder inhaler (DPI), (Aerolizer® DPI, Schering-Plough Co.), to generate the drug aerosols. The APS connected with the Aerolizer® DPI was operated at an inhalation flow rate of 30 L/min chosen to simulate actual patient use. The APS yields measurements of particle concentrations in the aerodynamic diameters (d_a) range of 0.57~20 μm. Each test by the APS was performed in triplicate and averaged. The true density of the particles (required as input to APS) was measured by a multipycnometer (Quantachrome, model MVP-1). The results based on averaging 5 measurements were 1.37±0.03 g/cm^3 for insulin/mannitol (IM) particles and 1.41±0.05 g/cm^3 for insulin/mannitol/trehalose (IMT) particles.

The theoretical aerodynamic diameter of a particle, d_a, is defined as the diameter of an equivalent spherical particle with a density of 1 g/cm^3 that has the same settling velocity as the particle of interest. It is the key particle property for characterizing respiratory deposition (24). Inhaled aerosols are typically described by the logarithm of the size distributions rather than the size itself because most aerosols exhibit a skewed distribution function with a long tail. Two important statistical properties of inhaled drug particles are the mass median aerodynamic diameter (MMAD) and the geometric standard deviation (GSD). MMAD can be directly calculated from the mass-based particle size distribution provided by APS. The GSD (σ_g) is obtained as:

$$\sigma_g = \sqrt{\frac{d_{a\,84\%}}{d_{a\,16\%}}}$$

where $d_{a\,84\%}$=the size associated with a cumulative count of 84% and $d_{a\,16\%}$=the size associated with a cumulative count of 16%.

To evaluate the effect of humidity, one particle sample was held at 37°C and 93% RH for 15 s, and a second sample held for 20 min. The particles were examined by SEM and APS and the results compared to those for the dry, freshly prepared particles.

Micro-Orifice Uniform Deposit Impactor

The aerosol performance of precipitated particles in particle transport within the respiratory tract was measured by MOUDI (MSP Co., model 110). The MOUDI operates at a fixed flow rate of 30 L/min and measures the aerodynamic particle size distribution within the size range of 0.32 to 18 μm in the inlet plus seven stages. The aerodynamic diameter ranges corresponding to the inlet and stages 1~7 are; >18, 18~10, 10~5.6, 5.6~2.5, 2.5~1.8, 1.8~1.0, 1.0~0.56, 0.56~0.32 μm, respectively. Particles deposited at the inlet and in stages 1 and 2 can be considered to be those that would deposit in the oropharyngeal region and stages 3, 4, 5 and 6 can be considered to correspond to the central and respiratory airways in the lung. The MOUDI was connected to an Aerolizer® DPI loaded with the drug particles. Each test using the MOUDI was performed in triplicate and the results averaged.

Fourier Transform Infrared Spectroscopy

FTIR spectroscopy analysis was used to monitor the structure of insulin before and after the ASES particle formation process. The FTIR measurements were conducted with a Genesis II (Mattson, model 960M0000) in the range 600~4,000 cm^{-1}, using a resolution of 2 cm^{-1} and 100 scans. Control of the instrument, as well as collection and primary analysis of data, was accomplished using WinFirst software (Mattson). Samples were diluted with KBr mixing powder at 1% and pressed with a KBr Die Kit and a hydraulic press (DAKE, model 44-226) to obtain self-supporting disks. Each insulin sample disk was measured at 3 different locations and the results averaged.

FTIR spectroscopy is frequently used to study structural characterization of proteins, particularly protein secondary structure. Thus conformational changes occurring during processing of the proteins can be detected using FTIR spectroscopy. In general, it has been suggested that amide I band (1,600~1,700 cm^{-1}) is more useful for protein secondary structure determination than amide II band (25). In order to assign secondary structures in the amide I band, Fourier self-deconvolution (FSD) was performed using OMNIC v 7.0 program (Thermo Electron Co.). A bandwidth of 15 cm^{-1} and enhancement factor of 2.5 were used for the FSD. FSD yields ten major peaks. The PeakFit v 4.11 program (SYSTAT Software Inc.) was used for curve fitting of the deconvoluted amide I band. Peaks were represented by Gaussian–Lorentzian functions.

Ultraviolet Spectroscopy

UV spectroscopy is useful for sample identification and quantitative measurements. The concentration of an analyte in solution can be determined by measuring the absorbance at

some characteristic wavelength. In this study, insulin concentration in solutions were determined using UV-Visible (Hewlett Packard, model HP 8453) tuned to the insulin characteristic frequency of 277 nm. An extinction coefficient of 0.95 cm^2 mg^{-1} was used.

X-ray Photoelectron Spectroscopy

XPS was used to determine whether insulin concentration on the particle surface is the same as the overall concentration. XPS is a surface analytical technique which measures the elemental composition of solid surface with an analyzed depth of about 5 nm. The XPS was performed using a Vacuum Generators Escalab MkII X-ray photoelectron spectrometer with a non-monochromatic Al Ka (1,486.6 eV) radiation source at a total power of 300 W. Spectral analysis and instrument control was performed using the VG5250 software. Survey scans were acquired at 1.0 eV per step intervals with a pass energy of 100 eV. Detailed scans of the C_{1S}, N_{1S}, and O_{1S} regions were acquired at 0.1 eV per step intervals with a pass energy of 20 eV. A sample area of approximately 2×10 mm diameter was analyzed. Binding energies were corrected for charging by referencing the C_{1S} signal of adventious carbonaceous contamination to a value of 285.0 eV.

X-ray Powder Diffraction

XRD was used to investigate the changes in the crystalline or amorphous nature of the components (insulin, mannitol and trehalose) in the particle formulation due to ASES processing. A sample was placed in aluminum holder (10×10 mm). The XRD scans were obtained on a Rigaku X-ray diffractometer with monochromatic Cu Kα radiation, generated by a 12 kW power supply and taken between 15° to 45° 2θ, with a step size of 0.02° per step, 4 s per step.

RESULTS AND DISCUSSION

Effect of Formulation on Particle Shape

Recently, several SCF technologies have been shown to be capable of producing microparticles of insulin (26–29). A few studies have been reported on the micronization of insulin particle for pulmonary delivery (22,26,28). In addition, from a practical point of view, insulin particles are generally micronized with additives such as stabilizers in order to improve physical and chemical characteristic of aerosol insulin. Thus, in this study, we first incorporated insulin with mannitol. Fig. 2a shows SEM pictures of insulin/mannitol (15/85 wt.%, IM) particles using *N*,*N*-dimethylformamide (DMF) as solvent at 35°C, 180 bar, 8 mg/mL solution concentration, and 5 ml/min solution flow rate. The particles formed were irregular and needle-shaped. Moderate changes in temperature/pressure and solution flow rate did not have significant effect on the particle morphology. Due to large surface area in needle-shaped particles, particle agglomeration is enhanced resulting in low deposition efficiency and poor dose reproducibility. The needle-shaped particles associated with the insulin/mannitol formulation are consistent with the results reported by Todo and co-workers (22) who showed that the insulin/mannitol particles agglomerated to each other. Since the needle shape is associated with mannitol

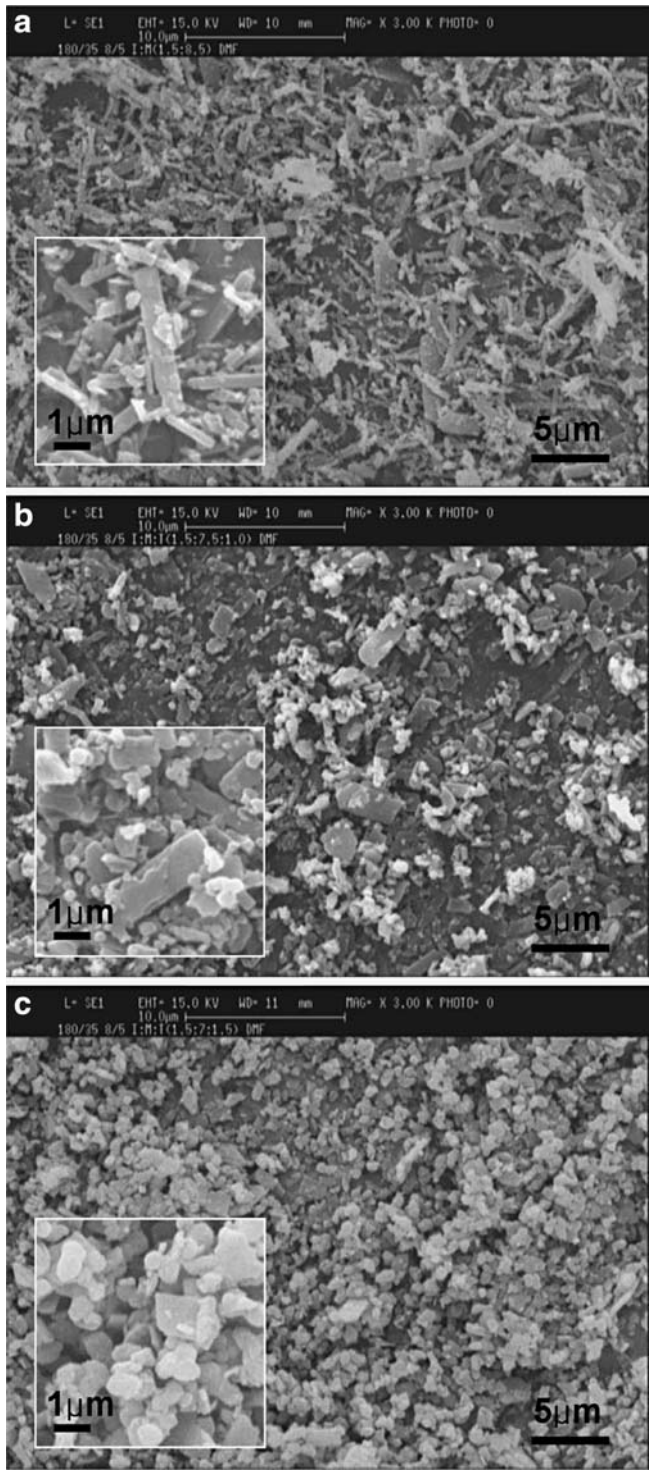

Fig. 2. SEM pictures of insulin with stabilizers particles precipitated from DMF at 35°C, 180bar, 8 mg/ml and 5 ml/min: **a** IM: insulin (15 wt.%), mannitol (85 wt.%), **b** insulin (15 wt.%), mannitol (75 wt.%), trehalose (10 wt.%), **c** IMT: insulin (15 wt.%), mannitol (70 wt.%), trehalose (15 wt.%), The *scale bars* represent 5 μm in *full images* and 1 μm in *insets*.

crystallization, we anticipate that the incorporation of an additive which does not crystallize in needle form would interfere with mannitol crystallization and result in more spherical particles. We added 10 and 15 wt.% trehalose which can also act as a stabilizer, but does not have mannitol's linear structure. SEM images of the particles formed are shown in Fig. 2b,c. Indeed we see that the particle shape became increasingly spherical as trehalose concentration was increased. We note that the choice of trehalose is based on three main considerations: first, like mannitol, trehalose has OH functional groups which act as stabilizer for insulin; second, due to chemical similarities, trehalose has high affinity for mannitol and thus is able to interfere with mannitol crystallization; and finally, trehalose's non linear molecular shape interferes with the formation of mannitol needles.

Effect of Solvent Choice

In our previous studies of particle formation in ASES processes, we found that solvent choice has great effect on particle size and morphology (30,31). Dimethylsulphoxide (DMSO) is a popular solvent for ASES particle formation. In this study, we compared DMSO and DMF as solvent in the formation of insulin particles. We have already shown above that using DMF as solvent can produce relatively spherical micron sized particles in an insulin/mannitol/trehalose (15/70/15 wt.%, IMT) formulation (Fig. 2c). We now vary the solvent by mixing DMSO and DMF in various proportions (0, 20, 30 and 100 vol.% DMSO). The solid particle formulation composition remained at 15% insulin, 70% mannitol and 15% trehalose by weight. The SEM images of the particles produced by varying the solvent are shown in Fig. 3. As the concentration of DMSO was increased, the shape of the particles became more needle-like, even though there was 15 wt.% of trehalose. It is primarily due to the different solubility of insulin in the solvents. Insulin has limited solubility in DMF but freely dissolves in DMSO. When DMF is used as solvent, the least soluble solute, insulin, precipitates first as the solution emerges from the nozzle and encounters supercritical CO_2. The particles grow by incorporating mannitol, trehalose and additional insulin. Because mannitol crystallizes easily and due to its higher concentration and smaller molecular weight (greater mobility), needle shaped crystals tend to form. When trehalose is present, the growth of mannitol needle shaped crystals is retarded because trehalose is chemically highly compatible with mannitol but

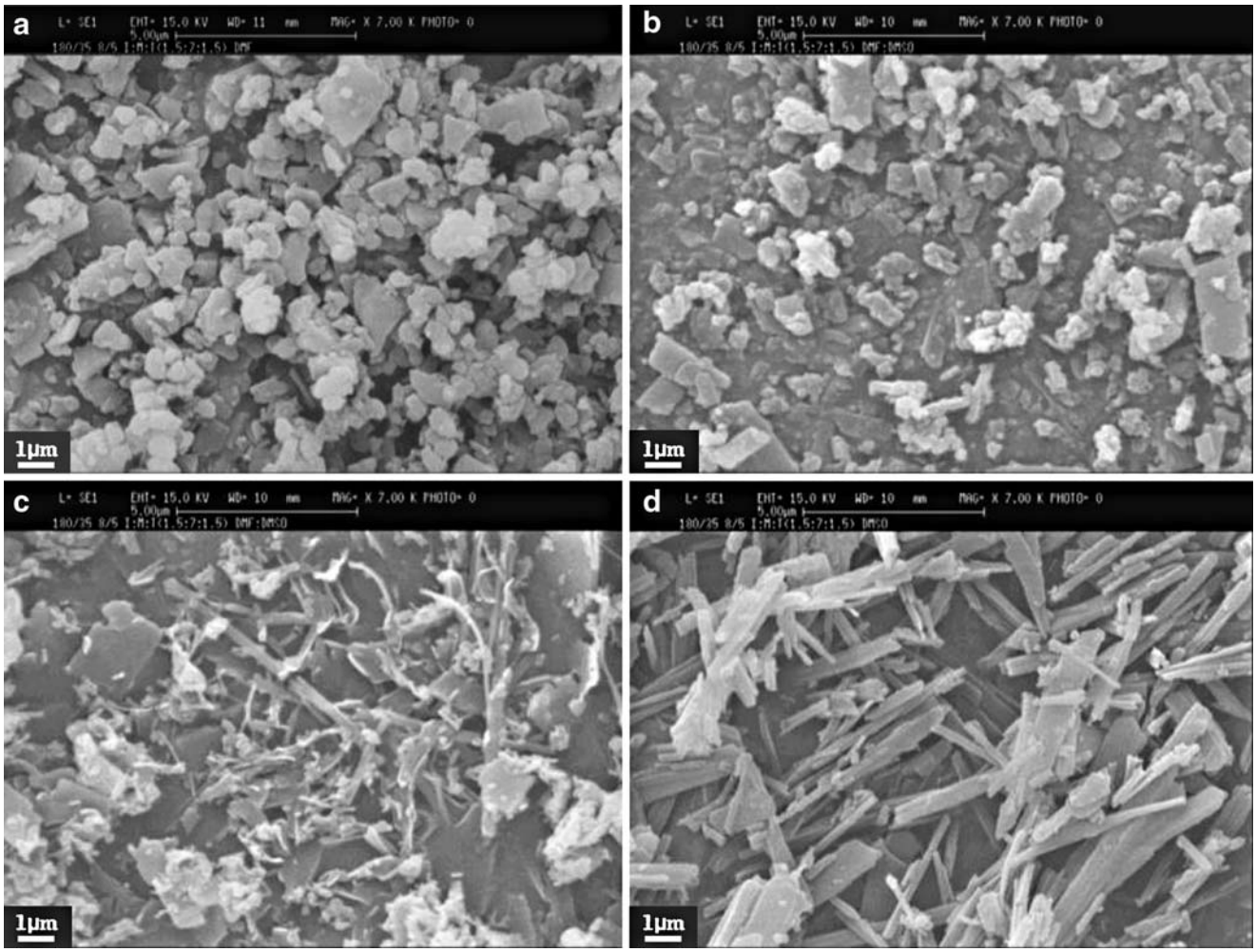

Fig. 3. SEM pictures of IMT particles obtained for different solvents at the same operating conditions, **a** DMF (100 vol.%)/DMSO (0 vol.%), **b** DMF (80 vol.%)/DMSO(20 vol.%), **c** DMF (70 vol.%)/DMSO (30 vol.%), **d** DMF (0 vol.%)/DMSO (100 vol.%).

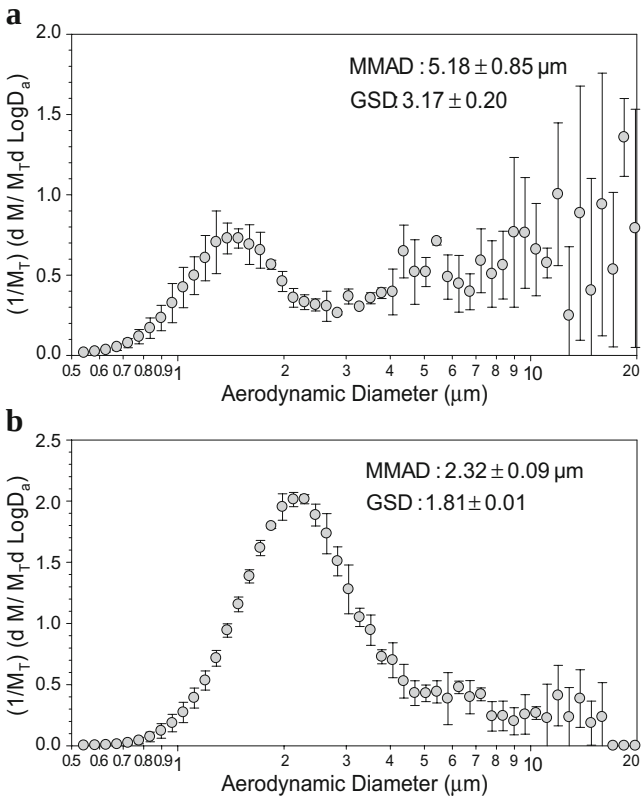

Fig. 4. Comparison of APS measured PSDs of insulin particles delivered from the Aerolizer® DPI at 30 L/min. **a** IM particles and **b** IMT particles.

different in molecular shape. DMSO is much less hydrophilic than DMF, so insulin is more soluble in DMSO than in DMF but mannitol and trehalose are less soluble in DMSO than in DMF. The crystallization rate of mannitol is therefore much higher in DMSO than DMF. So when the DMSO solution is injected into supercritical CO_2, the particles grow rapidly by incorporating mannitol preferentially because of its greater concentration and greater mobility relative to insulin and trehalose. The precipitation rates of insulin and trehalose in DMSO are not sufficiently high to interfere with the growth of the needle-shaped mannitol crystals. It is likely that a much higher concentration of trehalose would be necessary to interfere with the formation of needle-shaped mannitol crystals in DMSO.

Particle Size Distributions

Aerodynamic particle sizer (APS) was used for measurement of mass-based particle size distribution (PSD) and mass median aerodynamic diameter (MMAD) of the IM and IMT particles in an accelerating flow that simulates real-life inhalation flow conditions. Fig. 4 shows normalized PSDs of the IM particles with 0 and 15 wt.% trehalose obtained at a flow rate of 30 L/min. The needle shaped IM particles (Fig. 4a) showed highly irregular PSD pattern with a large relative standard deviation (RSD) of 16.4%. In general, particles of irregular or needle shape exhibit higher internal friction than more spherical particles due to increased contact area, leading to higher degree of particle agglomeration (14). In contrast, the more spherical IMT particles (Fig. 4b) showed a narrower PSD with a RSD of only 3.8%. The MMADs were calculated from PSDs. The MMADs of the IM and IMT particles were 5.18±0.85 and 2.32±0.09 μm, respectively. The respirable fraction (mass fraction in size range of 1 to 3 μm) for IMT particles is expected to be much higher than that for IM particles, resulting in much less waste (see next section). The narrower PSD is also expected to correspond to more consistent and reproducible deposition and therapeutic performance.

Aerosol Characteristics of Insulin Particles

Micro-Orifice Uniform Deposit Impactor (MOUDI) was used to quantify particle aerodynamic mass-weighted size distributions. Although MOUDI does not represent actual deposition fraction in different regions of human lung because losses within inhaler and environment before particles are passed into the mouth are not considered in this study, MOUDI can be used to estimate and compare deposition fraction of the produced drug particles within the respiratory tract. We compared the IM particles (Fig. 2a) and the IMT particles (Fig. 2c). The deposition fraction measured by MOUDI is shown in Fig. 5. It can be seen that without trehalose, most of the mass was recovered at the inlet and on stages 1 and 2 representing particle with diameters >18, 18~10, and 10~5.6 μm, respectively. Theses stages mostly represent the oropharyngeal regions. Most of the insulin in the particles deposited in these regions would be denatured or metabolized before reaching the circulatory system and hence non therapeutic. In contrast, a much smaller fraction of IMT particles was collected on the same stages. The particle deposition of the central and respiratory airways in the lung (the respirable fraction) is defined as the total mass fraction collected on stages 3, 4, 5 and 6 representing particle size with 5.6~2.5, 2.5~1.8, 1.8~1.0 and 1.0~0.56 μm, respectively. For efficient pulmonary delivery, the respirable fraction should be as high as possible. Quantitative comparisons based on the

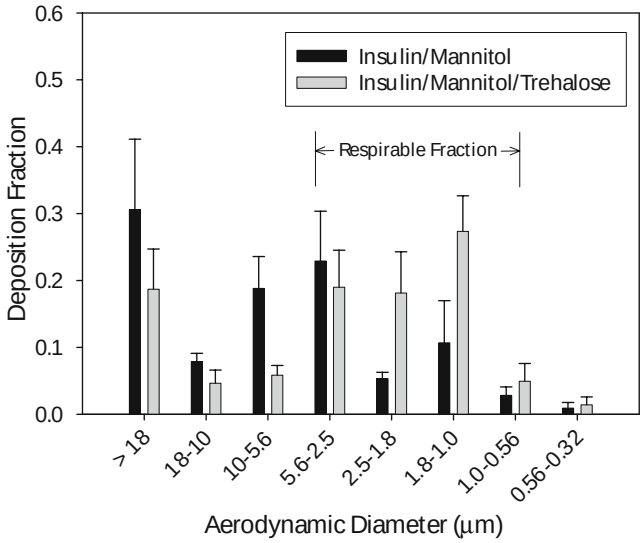

Fig. 5. *In vitro* aerosol performance of processed insulin particles measured by MOUDI.

Table I. Quantitative Comparisons of Non Respirable Fraction and Respirable Fraction in Terms of Total Mass Deposition and Insulin Concentration

	Non respirable fraction>5.6 μm			Respirable fraction 0.56~5.6 μm		
	Total mass fraction (wt.%)	Insulin fraction (%)	Average insulin concentration (%)	Total mass fraction (wt.%)	Insulin fraction (%)	Average insulin concentration (%)
IM	57±14	68±16	18±1	41±15	32±16	11±1
IMT	29±6	38±8	20±1	69±7	62±8	13±1

MOUDI results are shown in Table I where we see that the respirable particle deposition was 41±15 wt.% for the IM particle compared to 69±7 wt.% for the IMT particles. This highlights the result that adding trehalose enhances the inhalation performance of insulin particles and improves the particle deposition in the respiratory airways in the lung when compared to IM particles.

The therapeutic performance of the particles also depends on two additional particle properties: (1) the distribution of insulin within the particles (i.e., whether insulin is segregated on the particle surface, in the particle core or is uniformly distributed) and (2) whether this distribution changes with particle size. To answer the first question, we used XPS to examine the surface elemental composition of the particles (Fig. 6). Since only insulin contains nitrogen, presence of N peak in the XPS spectrum indicates insulin presence in the surface layer. If insulin concentration is uniform throughout the particle, from stoichiometry, the ratio of nitrogen atoms to carbon atoms in the XPS spectrum should be 0.25, 0.05 and 0.04 for pure insulin, IM particles and IMT particles respectively. The corresponding actual ratios observed from XPS are 0.19, 0.04 and 0.06, which are not vastly different from the stoichiometric ratios calculated based on the assumption of uniform distribution. So there was no significant evidence that insulin was preferentially segregated to either the interior or the surface regions of the particles. To address the second question, particles deposited in the inlet and stages 1 and 2 in the MOUDI (corresponding to particle sizes >5.6 μm) are combined and dissolved in 0.01 N HCl and examined using UV spectroscopy to measure the insulin concentration. The procedure was repeated for particles deposited in stages 3~6 corresponding to particle sizes 0.56 to 5.6 μm, (i.e., the respirable fraction). Comparison of IM and IMT particles are made and the results summarized in Table I. Table I shows that the IMT particles in the respirable size range contained 62±8% of total insulin, considerably higher than the IM

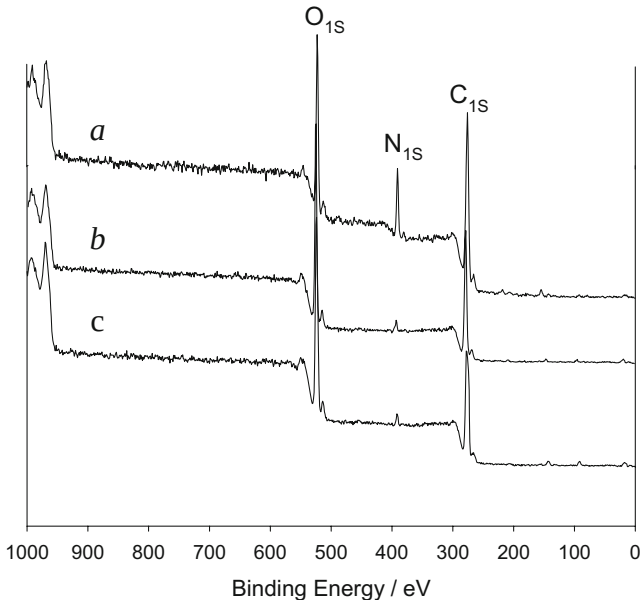

Fig. 6. Comparison of XPS spectra of insulin particles. *a* unprocessed insulin particles, *b* IM particles, *c* IMT particles.

Table II. Secondary Structures of Unprocessed and Processed Insulin with and Without Stabilizers from FTIR Spectroscopy

Sample	Tentative assignment										Total helix content
	S	i-H	S	U	α-H	3_{10}-H	S	S	T	T	
Unprocessed insulin											
Area (%)	5.2±0.6	9.7±1.4	6.9±0.0	11.4±1.2	10.7±0.9	15.4±0.1	10.1±0.1	9.7±0.1	9.8±0.8	11.3±0.6	35.8±0.4
Position (cm^{-1})	1,617±1	1,628±0	1,636±0	1,645±1	1,653±1	1,661±1	1,669±1	1,675±0	1,683±1	1,692±1	
Processed insulin (pure)											
Area (%)	6.4±1.4	8.1±0.4	6.0±0.6	14.7±0.8	11.7±0.6	14.6±0.7	9.7±0.8	8.9±0.8	8.6±1.3	11.4±2.3	34.4±0.6
Position (cm^{-1})	1,617±1	1,629±1	1,636±1	1,644±1	1,652±1	1,660±1	1,668±1	1,674±1	1,682±1	1,691±2	
Processed IM											
Area (%)	3.6±0.3	9.3±0.0	7.8±1.4	15.8±0.3	12.3±0.9	16.1±0.2	9.9±1.2	9.3±0.4	8.8±0.1	7.1±1.1	37.8±1.1
Position (cm^{-1})	1,617±0	1,628±0	1,636±0	1,645±1	1,653±1	1,661±1	1,669±1	1,675±0	1,683±1	1,692±1	
Processed IMT											
Area (%)	6.0±1.7	8.4±0.8	5.1±1.0	14.8±0.8	12.1±0.8	17.2±1.2	10.9±1.5	10.7±0.5	7.9±1.4	6.8±0.5	37.7±0.5
Position (cm^{-1})	1,616±2	1,629±1	1,635±2	1,644±1	1,651±1	1,660±1	1,668±1	1,675±1	1,683±1	1,692±1	

Data are mean value and standard deviation for three replicate measurements
S β-sheet, *i-H* irregular helix, *U* unordered, *α-H* α-helix, 3_{10}*-H* 3_{10}-helix, *T* β-turn, *IM* insulin/mannitol (15/85 wt.%) particles, *IMT* insulin/mannitol/trehalose (15/70/15 wt.%) particles

value of 32±16%. This means the IMT particles are much more efficient than IM particles in delivery insulin to the respiratory region. Table I also shows the calculated average insulin concentrations in the two fractions. If there is uniform distribution of insulin in particles of all sizes, then the value should be 15%. We see that the average insulin concentration in the respirable fraction was lower than 15%, for both IM and IMT particles, however the average insulin concentration in the IMT respirable fraction was slightly higher than in the IM case (13±1% *vs* 11±1%).

Secondary Structures of Insulin with Stabilizers

Since biological function of protein is sensitive to conformation, we used FTIR to determine whether ASES process affected the secondary structures of insulin. The assignments of the FTIR peaks to the secondary structures of insulin have been discussed by various authors and there are some differences in the assignment and number of peaks in the published literature (32–35). Most reports of bovine insulin secondary structure cite 8~10 peaks (32,34,35).

Table II shows the ten peaks identified from Fourier self-deconvolution of the FTIR spectra for the unprocessed pure insulin, pure insulin particles formed using the ASES process, IM and IMT particles. Also shown are integrated areas for each peak. The insulin amide I second-derivative infrared spectra of processed and unprocessed insulin particles are shown in Fig. 7. It is qualitatively obvious that the results showed that ASES processing did not significantly affect the insulin secondary structure. There is a small decrease in the total helical content (from 35.8±0.4% to 34.4±0.6%) when pure insulin was processed. However, when stabilizers (mannitol or trehalose) were added, the total helical content increased by about 3%. The helix structure is sensitive to hydrogen bonding (36) and therefore is often used as a measure of protein stability. So, the observed increase in helical content when mannitol and trehalose are added is consistent with the anticipated stabilizing role of these molecules.

Fig. 7. Second derivative infrared spectra in the amide I band for unprocessed and processed insulin.

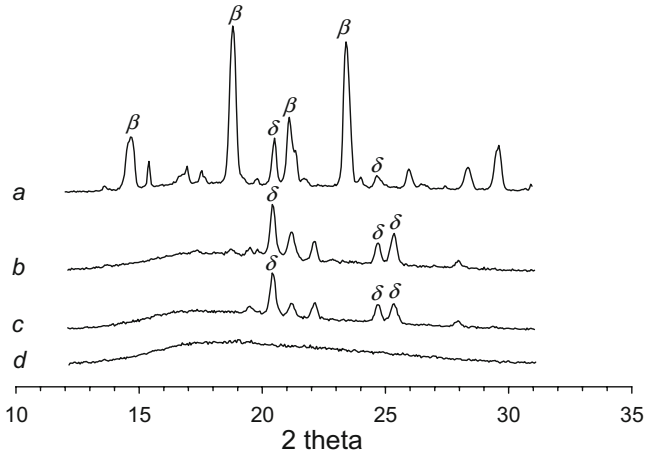

Fig. 8. Comparison of XRD scans of insulin particles. *a* Physical powder mixture of insulin with mannitol and trehalose (same proportions as in IMT particles), *b* IM particles, *c* IMT particles, *d* unprocessed pure insulin. β:β polymorph of mannitol (dominant peaks (Data from Powder Diffraction File (44))): 14.6°, 18.8°, 21.1° and 23.4°); δ:δ polymorph of mannitol (dominant peaks (Data from Powder Diffraction File (44)): 20.4°, 24.6° and 25.2°).

Crystallinity of Insulin Particles with Stabilizers

In many pharmaceutical products, crystallinity can affect storage stability and bioavailability (37–41). In this study, XRD was used to determine whether ASES processing affects the crystallinity of the various components in the formulation. Fig. 8 shows XRD scans for unprocessed pure insulin, physical mixture of unprocessed insulin (15 wt.%), mannitol (70 wt.%) and trehalose (15 wt.%) and processed insulin particles. Unprocessed insulin exhibited negligible crystallinity (Fig. 8(d)). Physical mixture of IMT exhibited strong crystallinity associated with the β polymorph of mannitol (Fig. 8(a)). Mannitol crystallinity was greatly reduced as result of ASES processing (Fig. 8(b) and (c)). Reduction in crystallinity is desirable in general because the amorphous form of the stabilizers such as mannitol and trehalose is preferred relative to the crystalline form since the amorphous molecules can form hydrogen bonds with the protein to preserve the protein native conformation and chemical stability (36,42,43).

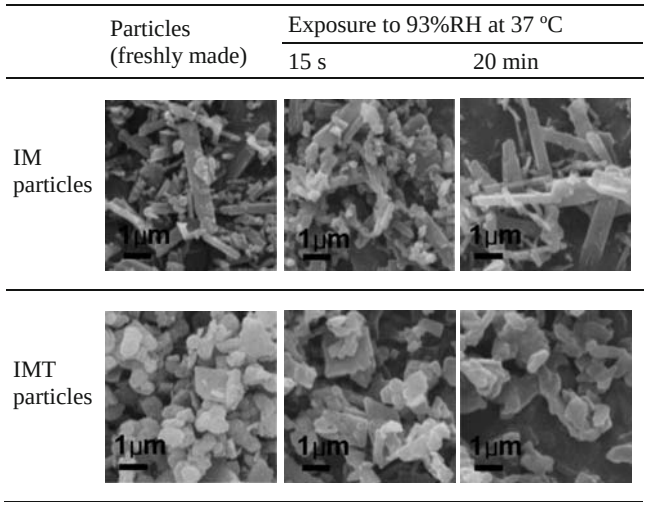

Fig. 9. SEM pictures of insulin with stabilizers particles exposed to high humidity for different times. Significant morphology variations observed after 20 min exposure to 93% RH.

Effect of High Humidity on Physical Characteristics of Insulin Particles

When exposed to moisture, mannitol and trehalose have a tendency to crystallize as well as to agglomerate. Agglomeration can significantly affect the aerodynamic behavior of the particles. In order to examine the effect of humidity on the micronized particles, we exposed the IM and IMT particles to 93%RH for 15 s and 20 min. The morphological changes were observed by SEM imaging, and the aerodynamic behavior was measured by APS. The SEM images are shown in Fig. 9. Morphological changes were not apparent at 15 s exposure to humidity, however, clear changes were observed at 20 min exposure, and for both IM and IMT particles exposed to humidity for 20 min, the PSDs could not be measured by APS because of high level of agglomeration. From a practical therapeutic point of view, the average residence time of the inhaled particles in the respiratory tract is less than 10 s. The APS results at 15 s exposure are shown in Fig. 10. When compared to the PSD of the freshly made particles (Fig. 4), clear difference can be observed for the IM

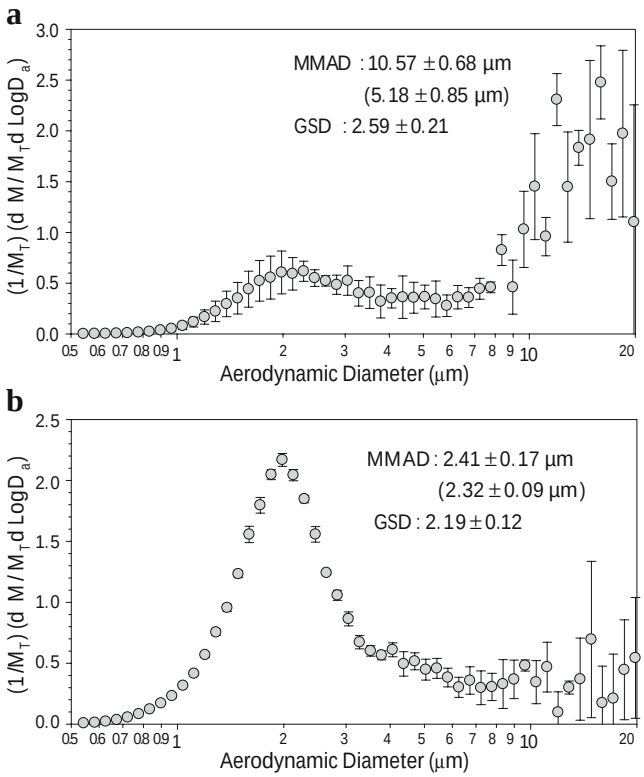

Fig. 10. Comparison of APS measured PSDs of insulin particles delivered from the Aerolizer® DPI at 30 L/min after 15 s exposure to 93% RH. **a** IM particles and **b** IMT particles. Quantities in *parenthesis* are for freshly made particles.

particles. The MMAD of the exposed IM particles evaluated from Fig. 10a was 10.57±0.68 μm, which is considerably larger than that for the freshly made particles (5.18±0.85 μm). This is probably due to the greater agglomeration tendency of the needle-shaped IM particles associated with the larger surface area. In contrast, the exposed IMT particles' MMAD of 2.41±0.17 μm is not significantly different from that of the freshly made IMT particles (2.32±0.09 μm). Therefore, the IMT particles are expected to show more reliable and more consistent particle deposition in the lung during inhalation compared to IM particles.

CONCLUSIONS

In this study, insulin particles suitable for pulmonary delivery were produced by an ASES process. The aerosol delivery efficiency was optimized by modifying the particle shape by means of varying the solvents, and by changing the nature and quantity of stabilizers. Two stabilizers, mannitol and trehalose, were used. The results indicated that insulin/mannitol/trehalose (IMT) particles produced by ASES process under appropriate conditions using DMF as solvent were relatively uniform, more spherical, less cohesive, and less agglomerated in an air flow, when compared to insulin/mannitol (IM) particles, which formed irregular and needle-shaped particles. The IMT particles were able to retain their PSD when exposed to high humidity conditions present in the respiratory tract during inhalation, while the IM particle MMAD almost doubled as a result of exposure to humidity. The secondary structures of insulin in the particles before and after the ASES processing were not significantly changed in either IM or IMT particles. XPS showed that there was no evidence that insulin was preferentially concentrated either in the interior or on the surface of the particles. MOUDI and UV spectroscopy results indicated that IMT particles deliver a much higher fraction of total insulin to the respiratory tract compared to IM particles.

In summary, the incorporation of trehalose to insulin and mannitol significantly improved the properties of the particles produced from the ASES process.

ACKNOWLEDGMENTS

Support from the WiSE program at USC is gratefully acknowledged.

REFERENCES

1. D. R. Owens, B. Zinman, and G. Bolli. Alternative routes of insulin delivery. *Diabet. Med.* **20**:886–898 (2003). doi:10.1046/j.1464-5491.2003.01076.x.
2. R. K. Wolff. Safety of inhaled proteins for therapeutic use. *J. Aerosol Med.* **11**:197–219 (1998).
3. J. Kling. Inhaled insulin's last gasp? *Nat. Biotechnol.* **26**:479–480 (2008). doi:10.1038/nbt0508-479.
4. W. T. Cefalu. Concept, strategies, and feasibility of noninvasive insulin delivery. *Diabetes Care* **27**:239–246 (2004). doi:10.2337/diacare.27.1.239.
5. J. S. Patton, J. Bukar, and S. Nagarajan. Inhaled insulin. *Adv. Drug Deliv. Reiv.* **35**:235–247 (1999). doi:10.1016/S0169-409X(98)00074-X.
6. D. R. Owens. New horizons-alternative routes for insulin therapy. *Nature Rev.* **1**:529–540 (2002).
7. R. U. Agu, M. I. Ugwoke, M. Armand, R. Kinget, and N. Verbeke. The lung as a route for systemic delivery of therapeutic proteins and peptides. *Respir. Res.* **2**:198–209 (2001). doi:10.1186/rr58.
8. S. J. Smith and J. A. Bernstein. Therapeutic uses of lung aerosols. In A. J. Hickey (ed.), *Inhalation Aerosols: Physical and Biologic Basis for Therapy*, Marcel Dekker, New York, 1996, pp. 233–269.
9. H.-C. Yeh, R. G. Cuddihy, R. F. Phalen, and I-Y. Chang. Comparisons of calculated respiratory tract deposition of particles based on the proposed NCRP model and the new ICRP66 model. *Aerosol Sci. Tech.* **25**:134–140 (1996). doi:10.1080/02786829608965386.
10. S. P. Velaga, R. Berger, and J. Carlfors. Supercritical fluids crystallization of budesonide and flunisolide. *Pharm. Res.* **19**:1564–1571 (2002). doi:10.1023/A:1020477204512.
11. B. Y. Shekunov, J. C. Feeley, A. H. L. Chow, H. H. Y. Tong, and P. York. Aerosolisation behaviour of micronised and supercritically-processed powders. *J. Aerosol Sci.* **34**:553–568 (2003). doi:10.1016/S0021-8502(03)00022-3.
12. M. Rehman, B. Y. Shekunov, P. York, D. Lechuga-Ballesteros, D. P. Miller, T. Tan, and P. Colthorpe. Optimisation of powders for pulmonary delivery using supercritical fluid technology. *Eur. J. Pharm. Sci.* **22**:1–17 (2004). doi:10.1016/j.ejps.2004.02.001.
13. E. Reverchon and A. Spada. Erythromycin micro-particles produced by supercritical fluid atomization. *Powder Technol.* **141**:100–108 (2004). doi:10.1016/j.powtec.2004.02.017.
14. H. Steckel, L. Pichert, and B. W. Müller. Influence of process parameters in the ASES process on particle properties of budesonide for pulmonary delivery. *Eur. J. Pharmaceut. Biopharmaceut.* **57**:507–512 (2004). doi:10.1016/j.ejpb.2004.01.002.
15. A. J. Hickey and C. A. Dunbar. A new millennium for inhaler technology. *Pharm. Technol.* **21**:116–125 (1997).
16. X. M. Zeng, G. P. Martin, and C. Marriott. *Particulate Interactions in Dry Powder Formulations for Inhalation*. Taylor & Francis, London, 2001, pp. 12–26.
17. B. Subramaniam, R. A. Rajewski, and K. Snavely. Pharmaceutical processing with supercritical carbon dioxide. *J. Pharm. Sci.* **86**:885–890 (1997). doi:10.1021/js9700661.
18. R. E. Sievers, U. Karst, P. D. Milewski, S. P. Sellers, B. A. Miles, J. D. Schaefer, C. R. Stoldt, and C. Y. Xu. Formation of aqueous small droplet aerosols assisted by supercritical carbon dioxide. *Aerosol Sci. Tech.* **30**:3–15 (1999). doi:10.1080/027868299304840.
19. F. Dehghani and N. R. Foster. Dense gas anti-solvent processes for pharmaceutical formulation. *Curr. Opin. Solid State Mater. Sci.* **7**:363–369 (2003). doi:10.1016/j.cossms.2003.11.001.
20. A. Shariati and C. J. Peters. Recent developments in particle design using supercritical fluids. *Curr. Opin. Solid State Mater. Sci.* **7**:371–383 (2003). doi:10.1016/j.cossms.2003.12.001.
21. S.-A. Cryan. Carrier-based strategies for targeting protein and peptide drugs to the lungs. *AAPS J.* **7**:E20–E41 (2005). doi:10.1208/aapsj070104.
22. H. Todo, K. Iida, H. Okamoto, and K. Danjo. Improvement of insulin absorption from intratracheally administrated dry powder prepared by supercritical carbon dioxide process. *J. Pharm. Sci.* **92**:2475–2486 (2003). doi:10.1002/jps.10497.
23. S. W. Stein, B. J. Gabrio, D. Oberreit, P. Hairston, P. B. Myrdal, and T. J. Beck. An evaluation of mass-weighted size distribution measurements with the model 3320 aerodynamic particle sizer. *Aerosol Sci. Tech.* **36**:845–854 (2002). doi:10.1080/02786820290092087.
24. W. C. Hinds. *Aerosol Technology-properties, Behavior, and Measurement of Airborne Particles*. 2nd ed., Wiley, New York, 1999, pp. 42–110.
25. M. Jackson and H. H. Mantsch. The use and misuse of FTIR spectroscopy in the determination of protein structure. *Crit. Rev. Biochem. Mol. Biol.* **30**:95–120 (1995). doi:10.3109/10409239509085140.
26. R. T. Bustami, H.-K. Chan, F. Dehghani, and N. R. Foster. Generation of micro-particles of proteins for aerosol delivery using high pressure modified carbon dioxide. *Pharm. Res.* **17**:1360–1366 (2000). doi:10.1023/A:1007551006782.
27. N. Elvassore, A. Bertucco, and P. Caliceti. Production of insulin-loaded poly(ethylene glycol)/poly(*l*-lactide) (PEG/PLA) nano-

particles by gas antisolvent techniques. *J. Pharm. Sci.* **90**:1628–1636 (2001). doi:10.1002/jps.1113.
28. W. Snavely, B. Subramaniam, R. Rajewski, and M. R. Defelippis. Micronization of insulin from halogenated alcohol solution using supercritical carbon dioxide as an antisolvent. *J. Pharm. Sci.* **91**:2026–2039 (2002). doi:10.1002/jps.10193.
29. N. Javanović, A. Bouchard, G. W. Hofland, G.-J. Witkamp, D. J. A. Crommelin, and W. Jiskoot. Stabilization of proteins in dry powder formulations using supercritical fluid technology. *Pharm. Res.* **21**:1955–1969 (2004). doi:10.1023/B:PHAM.0000048185.09483.e7.
30. Y. H. Kim and K. S. Shing. Supercritical fluid-micronized ipratropium bromide for pulmonary drug delivery. *Powder Technol.* **182**:25–32 (2008). doi:10.1016/j.powtec.2007.04.009.
31. Y. H. Kim, C. Sioutas, P. Fine, and K. S. Shing. Effect of albumin on physical characteristics of drug particles produced by supercritical fluid technology. *Powder Technol.* **182**:354–363 (2008). doi:10.1016/j.powtec.2007.06.008.
32. J. Wei, Y.-Z. Lin, J.-M. Zhou, and C.-L. Tsou. FTIR studies of secondary structures of bovine insulin and its derivatives. *Biochim. Biophys. Acta*. **1080**:29–33 (1991).
33. L. Xie and C.-L. Tsou. Comparison of secondary structures of insulin and proinsulin by FTIR. *J. Protein Chem.* **12**:483–487 (1993). doi:10.1007/BF01025049.
34. M. A. Winters, B. L. Knutson, P. G. Debenedetti, H. G. Sparks, T. M. Przybycien, C. L. Stevenson, and S. J. Prestrelski. Precipitation of proteins in supercritical carbon dioxide. *J. Pharm. Sci.* **85**:586–594 (1996). doi:10.1021/js950482q.
35. G. Vecchio, A. Bossi, P. Pasta, and C. Carrea. Fourier-transform infrared conformational study of bovine insulin in surfactant solutions. *Int. J. Pept. Protein Res.* **48**:113–117 (1996).
36. H.-K. Chan, A. R. Clark, J. C. feeley, M.-C. Kuo, S. R. Lehrman, K. Pikal-Cleland, D. P. Miller, R. Vehring, and D. Lechuga-Ballesteros. Physical stability of salmon calcitonin spray-dried powders for inhalation. *J. Pharm. Sci.* **93**:792–804 (2004). doi:10.1002/jps.10594.
37. M. J. Pikal and D. R. Rigsbee. The stability of insulin in crystalline and amorphous solids: observation of greater stability for the amorphous form. *Pharm. Res.* **14**:1379–1387 (1997). doi:10.1023/A:1012164520429.
38. B. Shenoy, Y. Wang, W. Shan, and A. L. Margolin. Stability of crystalline proteins. *Biotechnol. Bioeng.* **73**:358–369 (2001). doi:10.1002/bit.1069.
39. C. J. Roberts and P. G. Debenedetti. Engineering pharmaceutical stability with amorphous solids. *AIChE J.* **48**(6):1140–1144 (2002).
40. B. C. Hancock and M. Parks. What is the true solubility advantage for amorphous pharmaceuticals? *Pharm. Res.* **17**(4):397–404 (2000). doi:10.1023/A:1007516718048.
41. B. C. Hancock and G. Zografi. Characteristics and significance of the amorphous state in pharmaceutical systems. *J. Pharm. Sci.* **86**(1):1–12 (1997). doi:10.1021/js9601896.
42. J. F. Carpenter and J. H. Crowe. An infrared spectroscopic study of the interactions of carbohydrates with dried proteins. *Biochemistry.* **28**:3916–3922 (1989). doi:10.1021/bi00435a044.
43. T. Arakawa, S. J. Prestrelski, W. C. Kenney, and J. F. Carpenter. Factors affecting short-term and long-term stabilities of proteins. *Adv. Drug Deliv. Reiv.* **10**:1–28 (1993). doi:10.1016/0169-409X(93)90003-M.
44. Powder diffraction file. *Organic and Organometallic Phases*. JCPDS International Center for Diffraction Data, Swarthmore, 1987.